Electrochemical Investigation of 4-Hydroxy *n*-[2-Methoxy Naphthalene Methylidene] Benzohydrazide as Corrosion Inhibitor of Mild Steel in Acidic Medium

V. R. Adinarayanan[a], P. Preethi Kumari[a], and Suma A. Rao[a], *

[a] *Department of Chemistry, Manipal Institute of Technology, Manipal Academy of Higher Education, Manipal, 576104 India*
*e-mail: suma.rao@manipal.edu

Abstract—The corrosion rate of mild steel in hydrochloric acid and in sulphuric acid was determined by potentiodynamic polarization and electrochemical impedance spectroscopy in 0.5 M concentrations of HCl and of H_2SO_4 using 4-hydroxy *n*-[2-methoxy naphthalene methylidene] benzohydrazide (HNBH) as an inhibitor The inhibition efficiency of HNBH for the corrosion mitigation of mild steel was studied by varying the concentration of the inhibitor and temperature. It was found that the inhibition efficiency of HNBH increased with increase in the inhibitor concentration in both media. The maximum of 80% inhibition efficiency at the optimum inhibitor concentration of 2.5×10^{-4} M was achieved. However, with an increase in temperature, the inhibition efficiency decreased. The corrosion inhibition by HNBH took place through physisorption. The adsorption isotherm fitting with the experimental data was identified to find out the mechanism of inhibition. The results indicated that HNBH functions as mixed type inhibitor and follows the Langmuir adsorption isotherm. The surface of the specimen was analyzed using scanning electron microscopy.

Keywords: mild steel, acid corrosion, inhibition, impedance, polarization, physisorption, surface morphology

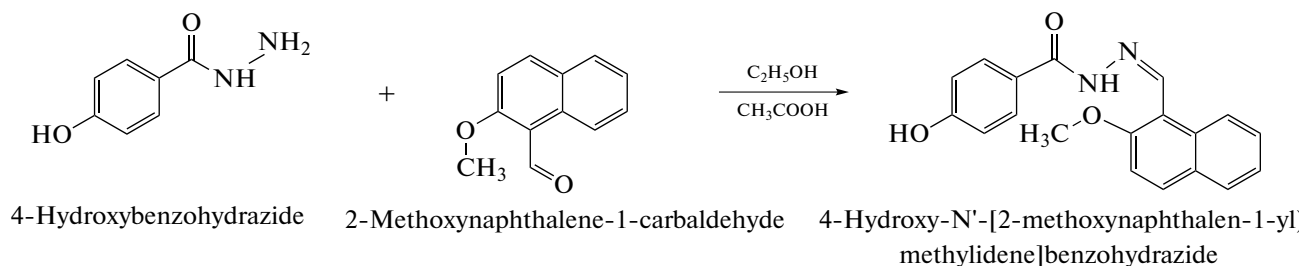**DOI:** 10.3103/S1068375522030024

INTRODUCTION

MS is a practical designing material by virtue of its properties, for example, strength, sturdiness, flexibility, machinability, and weld capacity. It finds applications in many of the everyday ordinary objects such as car body segments, motor cycle frames, cookware, as constructional material, in chemical reactors, boiler systems, storage tanks, oil and gas transport pipelines, etc. due to its excellent mechanical properties and low cost [1]. MS is utilized under different conditions including acidic environment wherein it undergoes degradation to some extent. The corrosion rate of the metal depends on the nature of the metal as well as on the environment. Acidic solutions are widely used for the expulsion of unwanted scale and rust. Among the economically available acids, the most often utilized are HCl and H_2SO_4. These acids are mainly used for pickling, cleaning, de-scaling, and acidization of oil [2]. As corrosion of MS is a significant issue, wherever process conditions permit, a suggested technique is addition of inhibitors to prevent the material loss [3]. A study of the mechanism of the action of corrosion inhibitors has importance both from the perspective of the quest for new inhibitors and also for their viable use. Most frequently cited in scientific literature are organic compounds containing nitrogen, oxygen, and sulphur because those compounds have heteroatoms, higher basicity and electron density. Heteroatoms and electron donating groups can form strong bonds on the surface of a metal, and hence act as good corrosion inhibitors [4, 5]. Despite the fact that various classes of heterocyclic compounds are being screened for their inhibitive activity, still there is a necessity to find new inhibitors. Hydrazide and its derivatives are attempted as corrosion inhibitors for metals. To mitigate the corrosion of MS in acidic media, the hydrazide derivatives [6−10], thiosemicarbazide derivatives, and acid hydrazide and hydrazone derivatives [11−14] are proposed because of the presence of electron donating groups, heteroatoms, π-electrons, and lone pairs of electrons in them. The planarity of the whole structure of the compounds dictates the formation of an adsorption film on a metal [15, 16].

The purpose of the present work was to investigate the corrosion inhibition of MS with the use of HNBH as corrosion inhibitor in 0.5 M concentrations of HCl and H_2SO_4.

Table 1. Composition of MS specimens

Element	C	Si	Mn	P	S	Cr	Ni	Mo	Al	Cu	Fe
wt %	0.169	0.188	0.414	0.060	0.042	0.020	0.028	0.018	0.004	0.072	Balance

4-Hydroxybenzohydrazide   2-Methoxynaphthalene-1-carbaldehyde   4-Hydroxy-N'-[2-methoxynaphthalen-1-yl, methylidene]benzohydrazide

Scheme 1. Synthetic route for preparation of HNBH.

EXPERIMENTAL

Material

The composition of the test coupons of MS used for the study is given in Table 1. MS specimens were embedded utilizing cold setting resin. The uncovered level surface (1 cm^2) of the mounted part was cleaned with emery papers of various grit levels and later disc polished with levigated alumina. The cleaned specimens were washed with double distilled water, rinsed with acetone, and dried before immersion in a corrosive medium.

Acidic Media

The solutions of 2 M HCl and H_2SO_4 acids were prepared using the A.R. grade acids (Merck) and distilled water. They were standardized by the volumetric method. The experiments were performed in the solutions of 0.5 M HCl and 0.5 M H_2SO_4 by the appropriate dilution of the stock solution. Experiments were done by adding 4 different concentrations of the inhibitor at three different temperatures: 303, 313, and 323 K.

Synthesis of HNBH

HNBH was synthesized as per reported literature [17]. An equimolar mixture of 2-methoxynaphthalene-1-carbaldehyde (0.01 mol) and 4-hydroxyl benzohydrazide (0.01 mol) dissolved in ethanol was refluxed on a hot water bath for about 5 h. The precipitated product was filtered, dried, and recrystallized from ethanol. The synthetic route for the preparation of HNBH is given in Scheme 1.

Characterization of Inhibitor

Characterization of HNBH was done by recording the Fourier transform infrared (FTIR) spectrum of HNBH with a spectrophotometer (Schimadzu FTIR 8400S) in a frequency range of 4000 to 400 cm^{-1} using KBr pellets. The FTIR spectrum of HNBH is given in Fig. 1.

FTIR (KBr) [cm^{-1}]: 3330 (OH *str.*), 3186 (NH *str.*), 3035 (Ar. CH *str.*), 1614(C=O), 1600(C=N *str.*), 1600 (Ar. C=C *str.*)

Electrochemical Measurements

Electrochemical measurements were performed utilizing an electrochemical work station (CH600D-series, U.S. Model with beta software). A customary three-electrode Pyrex glass cell with three electrodes was used: platinum as counter, calomel as reference, and MS as working electrodes. A cleaned MS test coupon was immersed in 100 mL of 0.5 M HCl without and with four different concentrations of HNBH at various temperatures (303, 313, and 323 K), and a steady state open circuit potential (OCP) was noted at the end of 300 s. The current vs. potential plots were recorded by polarizing the test coupon from −250 mV cathodically to +250 mV anodically, with respect to the OCP at a sweep pace of 0.1 mV s^{-1} and, from the plots, the corrosion potential (E_{corr}) and corrosion current density (i_{corr}) values were obtained [18]. The experiments were similarly carried out with 0.5 M H_2SO_4. The EIS tests were completed by applying an AC signal of 10 mV at a small amplitude in a frequency range of 100 kHz to 0.01 Hz, at the OCP. The impedance data were evaluated via Nyquist plots. PDP studies were performed immediately after EIS studies without further surface treatment.

Surface Characterization

The SEM images were recorded for the MS specimens corroded in each of 0.5 M HCl and H_2SO_4 with and without HNBH using an EVO 18-5-57 model microscope.
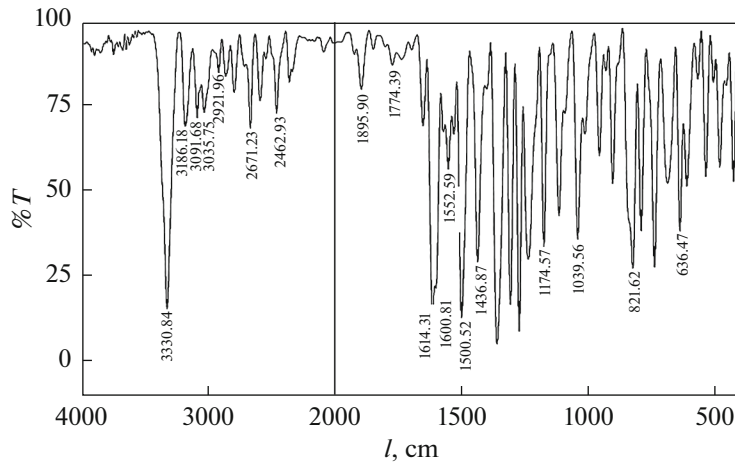
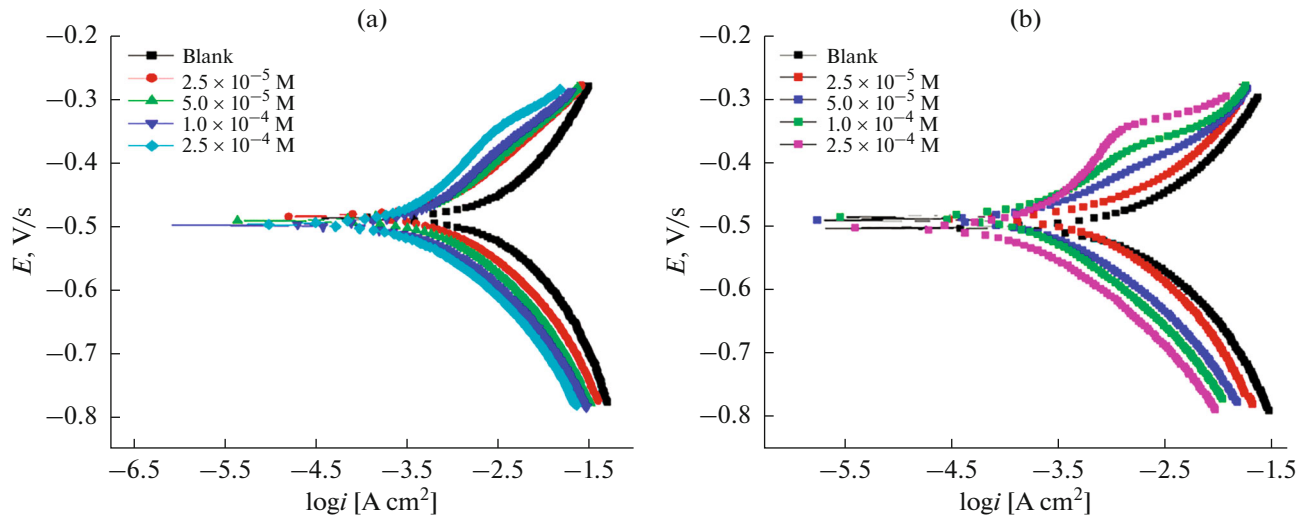**Fig. 1.** FTIR spectrum of HNBH molecule.

Fig. 2. PDP curves for MS specimens in: (a) 0.5 M HCl, and (b) 0.5 M H$_2$SO$_4$ at 303 K without and with various concentrations of HNBH.

RESULTS AND DISCUSSION

PDP Studies

PDP curves for MS without and with different concentrations of HNBH in 0.5 M HCl and H$_2$SO$_4$ solutions at 303 K are shown in Figs. 2a, 2b, respectively. Similar plots were recorded at different temperatures in both corrosive media. The values of the corrosion current density (i_{corr}), the corrosion potential (E_{corr}), the corrosion rate (CR), the anodic (β_a) and the cathodic Tafel slopes ($-\beta_c$), were recorded. The results are presented in Table 2.

The CR was determined using equation (1):

$$CR = \frac{3270 M i_{corr}}{\rho Z}, \quad (1)$$

where 3270 is a constant that defines the unit for the CR, M is the atomic mass of the metal (55.85), i_{corr} is the corrosion current density in A cm^{-2}, ρ is the density of the material (7.725 g cm^{-3}), and Z is the number of electrons transferred per metal atom ($Z = 2$) [19].

The percentage inhibition efficiency (IE%) of the inhibitor was determined using equation (2):

$$IE\% = \frac{i_{corr} - i_{corr(inh)}}{i_{corr}} \times 100, \quad (2)$$

where i_{corr} and $i_{corr(inh)}$ indicate the corrosion current density without and with the inhibitor, respectively. The surface coverage (θ) is associated with IE% as given in equation (3) [20]:

$$\theta = \frac{IE(\%)}{100}, \quad (3)$$

Table 2. Tafel polarization results for MS in 0.5 M HCl and 0.5 M H_2SO_4 without and with HNBH at different temperatures

Temp., K	HNBH (M)	0.5 M HCl			0.5 M H_2SO_4		
		i_{corr}, mA cm^{-2}	E_{corr}, mV	IE, %	i_{corr}, mA cm^{-2}	E_{corr}, mV	IE, %
303	0	1.053	−499	–	1.259	−499	–
	2.5×10^{-5}	0.267	−487	74.60	0.740	−486	41.21
	5×10^{-5}	0.214	−483	79.71	0.342	−487	72.86
	1×10^{-4}	0.184	−480	82.52	0.191	−483	84.81
	2.5×10^{-4}	0.143	−477	86.45	0.184	−485	85.38
313	0	1.456	−489	–	1.840	−497	–
	2.5×10^{-5}	0.421	−488	71.06	1.166	−488	36.61
	5×10^{-5}	0.354	−476	75.66	0.618	−484	66.44
	1×10^{-4}	0.320	−474	78.03	0.360	−486	80.45
	2.5×10^{-4}	0.251	−473	82.76	0.310	−485	83.16
323	0	2.790	−487	–	2.406	−497	–
	2.5×10^{-5}	0.848	−485	69.60	1.935	−493	19.58
	5×10^{-5}	0.774	−480	72.27	1.122	−487	53.36
	1×10^{-4}	0.675	−474	75.79	0.592	−495	75.40
	2.5×10^{-4}	0.585	−470	79.03	0.476	−490	80.20

From Table 2, given below, it can be observed that, in the absence of HNBH, the corrosion current density (i_{corr}) increased with an increase in temperature, which resulted in an increase in the CR. The IE% increased with an increase in the inhibitor concentration at each of the temperature (303, 313, and 323 K) studied in both 0.5 M HCl and H_2SO_4. The maximum IE of 85% was obtained at the optimum inhibitor concentration of 2.5×10^{-4} M. An increase in IE% with an increase in the inhibitor concentrations is due to the blocking effect of the metal surface by adsorption or film formation or both. In each of 0.5 M HCl and H_2SO_4, it was seen that the inhibition efficiency decreased with increase in temperature at all levels of HNBH addition. There was no remarkable shift in E_{corr} with the addition of HNBH in both acidic media with respect to the uninhibited one. As reported in literature, if the shift in the OCP in the presence of an inhibitor exceeds ±85 mV with respect to the corrosion potential of the uninhibited solution, then the inhibitor functions as either anodic or cathodic type [21, 22].

In the present case, the maximum displacement in E_{corr} was well within +20 mV, which means that HNBH acted as mixed type inhibitor. There was no appreciable change in the Tafel slopes (anodic slope or cathodic slope) with an increase in the inhibitor concentration. This indicated that the mechanism of the anodic and/or cathodic reaction did not alter with an increase in the inhibitor concentration [23]. The

obtained result was similar to the inhibition efficiency reported in the study of the corrosion inhibition of MS and carbon steel in HCl [7, 8], respectively.

EIS Studies

The impedance responses of the corrosion behavior of MS in the absence and the presence of the inhibitor were given in terms of the Nyquist plots (see Figs. 3a, 3b). The plots were obtained with depressed semicircles whose diameters increased with an increase in the inhibitor concentration. This shows that the charge transfer process is mostly controlling the corrosion of MS [24]. The depressed capacitive behavior can be credited to the contribution from roughness of the metal surface, active sites distribution, or inhibitor adsorption [25]. The Nyquist plots for the corrosion inhibition of MS in the presence of the inhibitor consisted of one distorted capacitive loop at a higher frequency due to the charge transfer reaction and the time constant of the electric double layer [26].

The impedance parameters were analyzed by fitting suitable equivalent circuits using a ZSimpWin software version 3.21. Simple Randles equivalent circuits (see the inserts in Figs. 4a, 4b) were used to fit the Nyquist plots in the absence and the presence of the inhibitor in 0.5 M HCl and H_2SO_4 solutions. The circuit in Fig. 4a, model: $R(QR)$, consisted of the solution resistance R_s, the charge transfer resistance R_{ct},
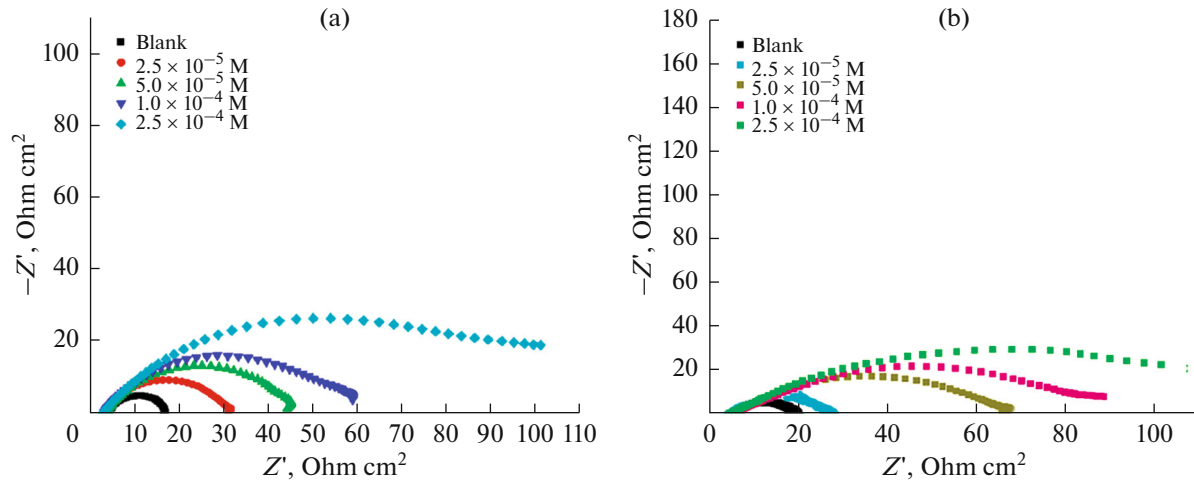
Fig. 3. Nyquist plots for MS specimens in: (a) 0.5 M HCl, and (b) 0.5 M H_2SO_4 containing HNBH at 303 K.
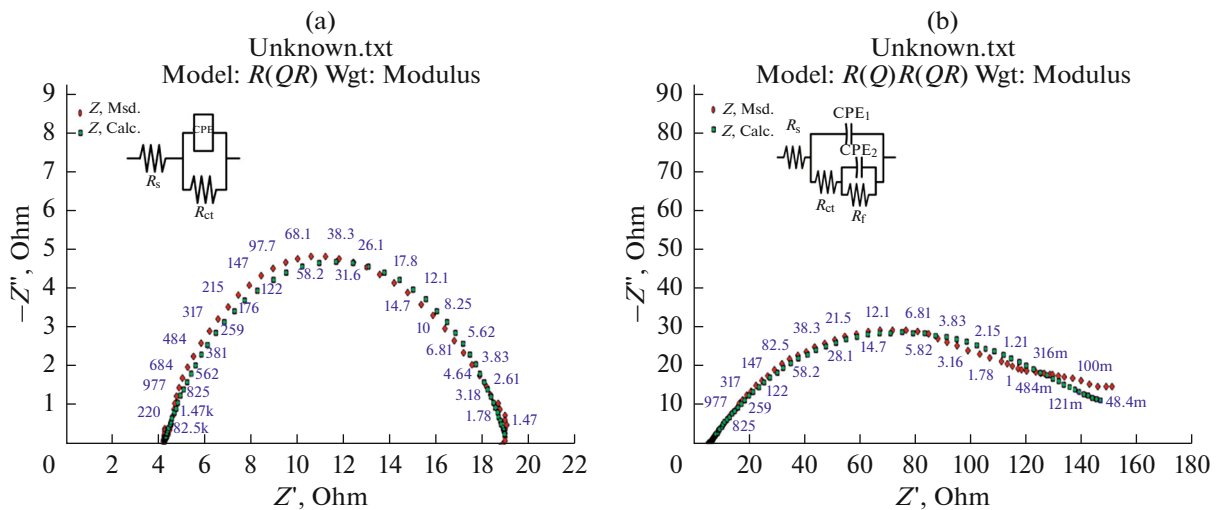

Fig. 4. Equivalent circuits (inserts) used to fit experimental EIS data for corrosion of MS with HNBH in: (a) 0.5 M HCl and (b) 0.5 M H_2SO_4.

and CPE. A CPE was employed instead of the double-layer capacitance C_{dl} to describe the heterogeneity in the system [26]. The circuit in Fig. 4b, model: $R(Q)R(QR)$, contained the solution resistance (R_s), the charge transfer process (R_{ct}), the time constant electrical double layer (CPE$_1$), the capacitance of the surface film (CPE$_2$), and the film resistance (R_f). The CPE behaves like an ideal double-layer capacitance (C_{dl}) and is calculated from frequency (f_{max}) at which the imaginary component of impedance was maximum using equation (4):

$$C_{dl} = \frac{1}{2\pi R_{ct} f_{max}}. \tag{4}$$

The results of EIS parameters are recorded in Table 3.

An increase in the inhibitor concentration tends to reduce the double layer capacitance due to the replacement of the adsorbed water molecule from the metal surface by the adsorbed inhibitor molecule thereby reducing an active surface area by a protective film. Further reduction in C_{dl} was credited to increase the thickness of the electrical double layer at the metal–solution interface [27]. It is evident from Table 3 that the measured C_{dl} values decreased with an increase in the inhibitor concentration in the case of both 0.5 M HCl and H_2SO_4 solutions used and at all three temperatures. A decrease in C_{dl} can be attributed to an increase in the thickness of the electrical double layer at the metal–solution interface and a gradual replacement of water molecules by the adsorption of inhibitor molecules on the metal surface [27]. An increase in the

Table 3. EIS data for MS in 0.5 M HCl and 0.5 M H$_2$SO$_4$ without and with different concentrations of HNBH at different temperatures

Temp, K	HNBH, M	0.5 M HCl			0.5 M H$_2$SO$_4$		
		C_{dl}, µF cm^{-2}	R_{ct}, Ω cm^2	IE, %	C_{dl}, µF cm^{-2}	R_{ct}, Ω cm^2	IE, %
303	0	2539	15.00	0	1514	16.14	0
	2.5×10^{-5}	309	53.17	71.78	984	27.23	40.72
	5×10^{-5}	182	65.03	76.93	171	52.36	69.17
	1×10^{-4}	127	73.24	79.51	79	90.14	82.09
	2.5×10^{-4}	57	102.0	85.29	54	96.38	83.25
313	0	3056	12.24	0	3969	10.49	0
	2.5×10^{-5}	381	42.10	70.92	1769	15.45	31.10
	5×10^{-5}	233	50.23	75.63	66	30.58	65.69
	1×10^{-4}	172	55.04	77.76	22	46.28	77.33
	2.5×10^{-4}	111	67.20	81.78	13	53.36	80.34
323	0	7395	8.63	0	5036	8.474	0
	2.5×10^{-5}	907	27.00	68.03	3787	10.26	17.44
	5×10^{-5}	702	31.00	72.16	1692	17.68	52.09
	1×10^{-4}	580	32.21	73.20	378	34.08	75.14
	2.5×10^{-4}	342	37.89	77.22	244	38.27	77.86

R_{ct} values in the presence of different concentrations of HNBH results in the reduction in the CR because of the formation of an adsorbed protective film on the metal−solution interface. The results obtained via both PDP and EIS methods were in good agreement at all the studied temperatures.

The charge transfer resistance is a measure of resistance against electron transfer across the surface, and it is inversely proportional to the CR, which was used to calculate the IE(%) via equation (5):

$$IE\,(\%) = \frac{R_{ct(inh)} - R_{ct}^0}{R_{ct(inh)}}, \qquad (5)$$

where $R_{ct(inh)}$ and R_{ct}^0 are the charge transfer resistances with and without the inhibitor. From Table 3 it is seen that an increase in the inhibitor concentration results in a higher R_{ct} value, which specified that the corrosion process is mainly controlled by the charge transfer process.

Effect of Temperature

The influence of temperature on the CR of MS and %IE of HNBH was studied at three different temperatures: 303, 313, and 323 K. It can be seen from Table 2 that the addition of the inhibitor reduced the CR. As to the inhibition efficiency, it was found to decrease

with an increase of temperature. This is because of a highly aggressive nature of the acids, which overcomes the inhibitory action of the inhibitor at higher temperature, additionally as the temperature rises, the adsorbed inhibitor molecules get desorbed from the metal surface resulting in the reduction in the inhibition efficiency [28, 29].

The Arrhenius equation (6) is used to calculate the activation energy (E_a) for the corrosion process:

$$\ln(CR) = B - \frac{E_a}{RT}, \qquad (6)$$

where B is called the Arrhenius pre-exponential constant, R is the universal gas constant, and T is the temperature.

The slopes obtained from the plots of ln(CR) vs. $1/T$ shown in Figs. 5a, 5b were used to calculate the activation energy for the corrosion and the inhibition processes [28]. The enthalpy of activation (ΔH_a) and the entropy of activation (ΔS_a) for the metal dissolution process were found out using the transition state equation (7):

$$CR = \frac{RT}{Nh} \exp\left(\frac{\Delta S^{\#}}{RT}\right) \exp\left(\frac{-\Delta H^{\#}}{RT}\right), \qquad (7)$$

where h is Planck's constant and N is Avogadro's number. Plots of ln(CR/T) vs. $1/T$ (Figs. 6a, 6b), are straight lines with the slope $-\Delta H_a/T$ and the intercept
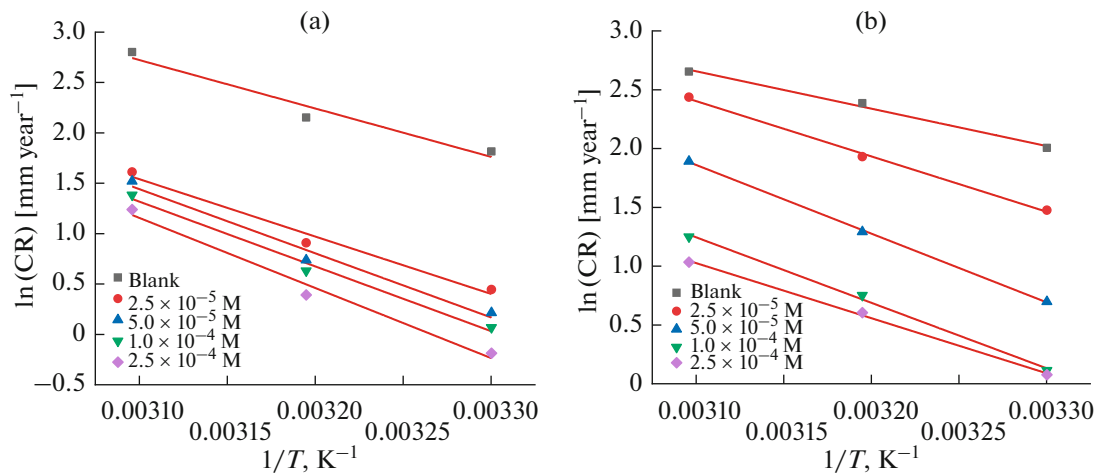
Fig. 5. Plots of ln(CR) vs. (1/T) for MS in: (a) 0.5 M HCl, and (b) 0.5 M H$_2$SO$_4$, without and with various inhibitor concentrations.

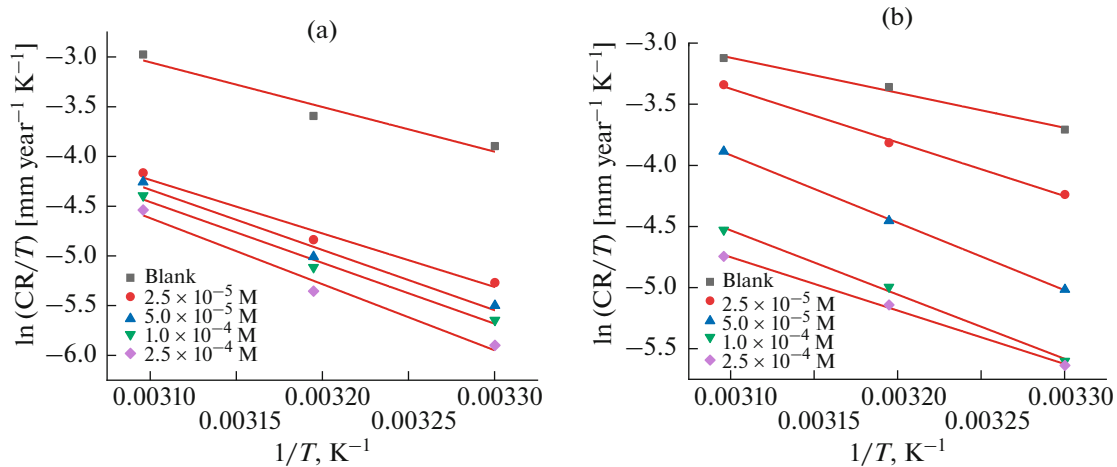**Fig. 6.** Plots of ln(CR/T) vs 1/T for MS in: (a) 0.5 M HCl and (b) 0.5 M H$_2$SO$_4$ without and with various concentrations of HNBH.

ln(R/Nh) $+\Delta S_\mathrm{a}/R$. The activation parameters for MS in 0.5 M HCl and in H$_2$SO$_4$ were obtained and recorded in Table 4.

An increase in the activation energy with an increase in the inhibitor concentration shows an increase in the energy barrier for the corrosion reaction and signifies that adsorption of the inhibitor takes place through physisorption in both 0.5 M HCl and 0.5 M H$_2$SO$_4$ [30]. A negative value of the entropy of activation indicates that there is a decrease in randomness on going from reactants to the activated complex [31].

Table 4. Activation parameters for corrosion of MS in 0.5 N HCl and 0.5 M H$_2$SO$_4$ with various concentrations of HNBH

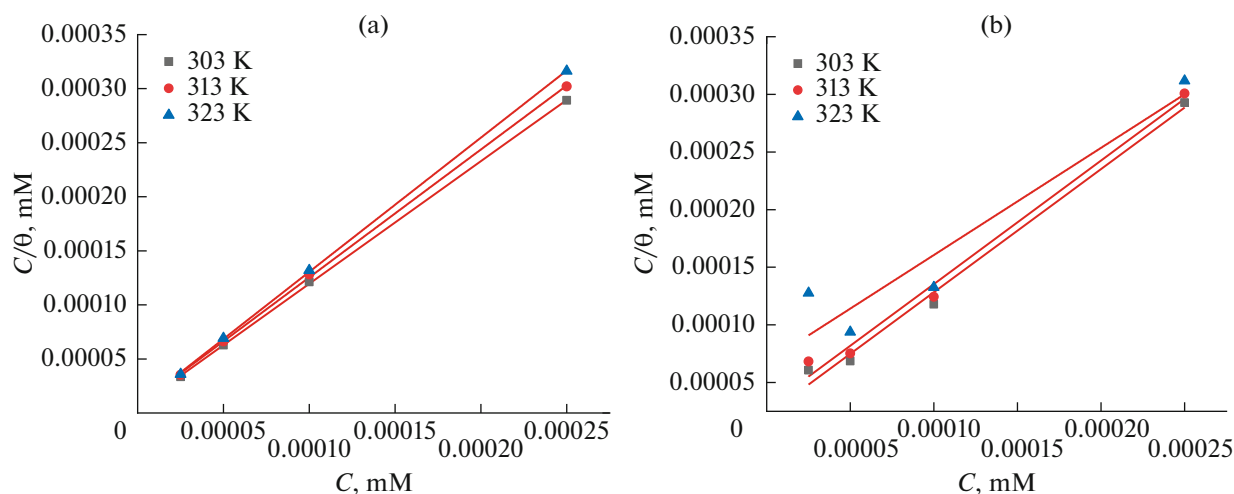| HNBH, M	0.5M HCl			0.5M H$_2$SO$_4$		
	E_a, kJ mol^{-1}	ΔH, kJ mol^{-1}	$-\Delta S^{\neq}$, J mol^{-1} K^{-1}	E_a, kJ mol^{-1}	$\Delta H^{\neq}$, kJ mol^{-1}	$-\Delta S^{\neq}$, J mol^{-1} K^{-1}
0	39.92	37.32	107.19	26.39	23.79	93.6
2.5×10^{-5}	47.27	44.67	94.24	39.06	36.46	56.43
5×10^{-5}	52.65	50.05	78.39	48.36	45.76	32.12
1×10^{-4}	53.23	50.63	77.61	46.01	43.41	44.52
2.5×10^{-4}	57.7	55.10	65.09	38.72	36.12	68.96

Fig. 7. Langmuir adsorption isotherms of MS in: (a) 0.5 M HCl and (b) 0.5 M H$_2$SO$_4$.

Adsorption Considerations

Adsorption isotherms give the information about the interaction among an inhibitor and a metal surface, which assists in understanding the mechanism of corrosion inhibition. HNBH adsorbs on the metal surface and forms a film over it thus isolating the metal surface from the action of the medium. The estimation of θ at various concentrations of HNBH has been utilized to describe a few isotherms to fit the adsorption process. In the temperature range considered, the Langmuir adsorption isotherm was found to fit best, and it is given by equation (8):

$$\frac{C_{inh}}{\theta} = \frac{1}{K} + C_{inh},$$ (8)

where K is the equilibrium constant for the metal–inhibitor interaction, C_{inh} is the inhibitor concentration, and θ is the degree of the surface coverage [32].

The plots of C_{inh}/θ vs. C_{inh} for different temperatures provide straight lines with the intercept $1/K$ as shown in Figs. 7a, 7b for 0.5 M HCl and H$_2$SO$_4$, respectively. The values of the standard free energy of adsorption are related to K by relation (9):

$$K = \frac{1}{55.5} \exp\left(\frac{-\Delta G_{ads}^{\circ}}{RT}\right),$$ (9)

where R is the universal gas constant, T is the absolute temperature, and 55.5 is the concentration of water in a solution in mol dm^{-3} [33]. The isotherm that best fits the experimental data was chosen using the correlation coefficient (R^2). The correlation coefficient values were close to unity as shown in Table 5. A slight deviation of the slopes of straight lines from a unity shows that the adsorption of HNBH obeys the Langmuir adsorption isotherm.

The plot of ΔG_{ads}^{0} vs T for the adsorption of HNBH on mild steel in 0.5M HCl and 0.5 M H$_2$SO$_4$ is shown in Fig. 8. The standard enthalpy of adsorption (ΔH_{ads}^{0}) and the standard entropy of adsorption (ΔS_{ads}^{0}) were computed from the slope and the intercept of the straight line, respectively, according to the thermodynamic equation (10):

$$\Delta G_{ads}^{0} = \Delta H_{ads}^{0} - T\Delta S_{ads}^{0}.$$ (10)

Generally, the values of ΔG_{ads}^{0} around −20 kJ mol^{-1} or lower are consistent with physisorption, while those

Table 5. Thermodynamic parameters for adsorption of HNBH on MS in 0.5 M HCl and 0.5 M H$_2$SO$_4$

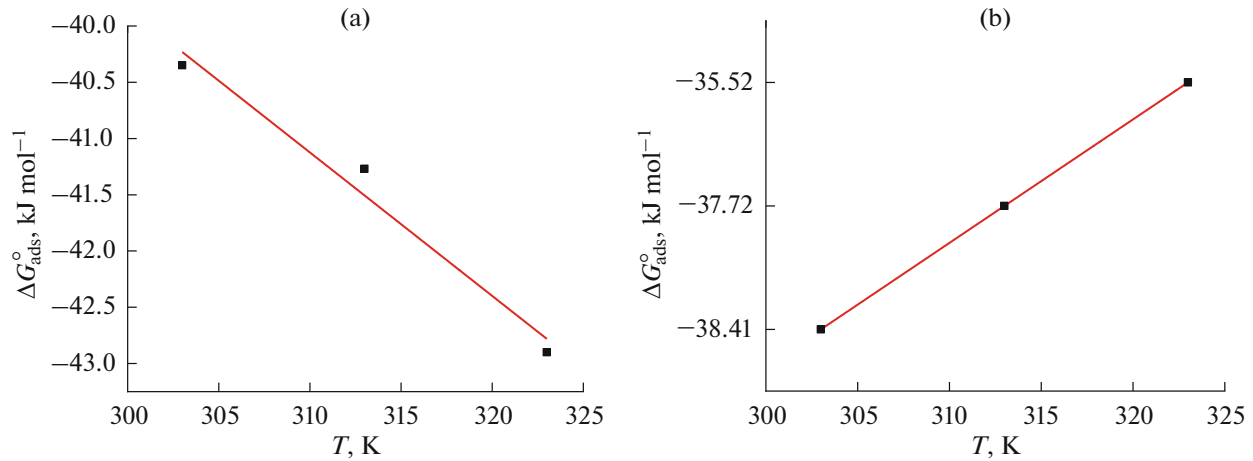| Temp, K	0.5 M HCl $R^2 = 0.9740$			0.5 M H$_2$SO$_4$ $R^2 = 0.9765$		
	ΔG_{ads}^{0}, kJ mol^{-1}	ΔH_{ads}^{0}, kJ mol^{-1}	ΔS_{ads}^{0}, kJ mol^{-1} K^{-1}	ΔG_{ads}^{0}, kJ mol^{-1}	ΔH_{ads}^{0}, kJ mol^{-1}	ΔS_{ads}^{0}, kJ mol^{-1} K^{-1}
303	−40.35			−38.41		
313	−41.27	−78.83	−0.127	−37.72	−82.44	−0.144
323	−42.90			−35.52		

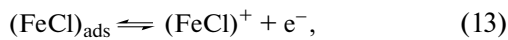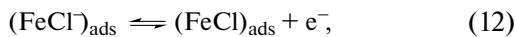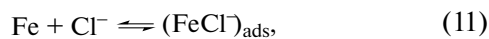**Fig. 8.** Plots of ΔG_{ads}^{0} vs. T for adsorption of HNBH on MS in: (a) 0.5 M HCl, and (b) 0.5 M H_2SO_4.

around 40 kJ mol^{-1} or higher are chemisorption [34]. It is observed from Table 5 that the ΔG_{ads}^{0} values in 0.5 M HCl and H_2SO_4 were found to be between -35 and -45 kJ mol^{-1}. This indicates the mixed adsorption behavior of HNBH on the MS surface, but the negative values of ΔH_{abs}^{0} strongly suggest that the physisorption of HNBH is exothermic. The ΔS_{ads}^{0} values are found to be negative suggesting a decrease in disorderness from the reactant to the adsorbed species [35].
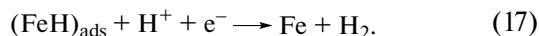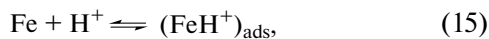
Corrosion Inhibition Mechanism

The main considerations that impact the adsorption of inhibitors are the nature of the metal surface, the chemical structure of the inhibitor, the distribution of charge in the molecule, the type of the aggressive electrolyte, and the type of interaction between the inhibitor molecules and the metallic surface. The dissolution of MS in an acidic solution takes place as demonstrated below.

At anodic region:

$$Fe + Cl^- \rightleftharpoons (FeCl^-)_{ads}, \quad (11)$$

$$(FeCl^-)_{ads} \rightleftharpoons (FeCl)_{ads} + e^-, \quad (12)$$

$$(FeCl)_{ads} \rightleftharpoons (FeCl)^+ + e^-, \quad (13)$$

$$(FeCl)^+ \rightleftharpoons Fe^{2+} + Cl^-. \quad (14)$$

The major cathodic reactions take place is the hydrogen gas evolution:

$$Fe + H^+ \rightleftharpoons (FeH^+)_{ads}, \quad (15)$$

$$(FeH^+)_{ads} + e^- \longrightarrow (FeH)_{abs}, \quad (16)$$

$$(FeH)_{ads} + H^+ + e^- \longrightarrow Fe + H_2. \quad (17)$$

The adsorption of the inhibitor molecule is a kind of a diplacement reaction involving the removal of adsorbed water molecules from the metal surface [36]:

$$Inh_{(sol)} + nH_2O_{(ads)} \rightleftharpoons Inh_{(ads)} + nH_2O_{(sol)}. \quad (18)$$
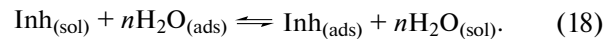
As reported in literature, Cl^- can get more effectively adsorbed than SO_4^{2-} [37]. The surface charge of MS at the OCP is positive in both inhibited and uninhibited 0.5 M HCl and 0.5 M H_2SO_4 media with respect to the potential of zero charge [38]. In a corrosive medium (for example 0.5 M HCl or 0.5 M H_2SO_4), HNBH gets protonated and forms positively charged species. These charged inhibitor molecules cannot approach the positively charged metal surface because of electrostatic repulsion. However, the anions of the acids can get attached to the metal surface. Because of this, the chloride and sulfate ions are adsorbed first at the interface by electrostatic forces. Therefore, the charge of the solution side changes from positive to negative, and the protonated inhibitor molecules are pulled in towards the negative charge, which encourages the adsorption of HNBH. Consequently, the protonated HNBH molecules will electrostatically adsorb on the MS surface through the chloride and sulfate, indicating physisorption. These protonated HNBH molecules can likewise be adsorbed at the cathodic areas of the metal in competition with the hydrogen ions, and, in this manner, they can decrease the rate of liberation of hydrogen [39, 40].

Surface Characterization

The SEM pictures of surface of MS dipped in 0.5 M HCl and 0.5 M H_2SO_4 solutions for 3 h (both in the uninhibited and with HNBH) were taken. The uneven surface with pits and breaks demonstrate the uniform corrosion of the sample. The SEM pictures of MS samples immersed in 0.5 M HCl and in 0.5 M H_2SO_4 containing 25 mL of HNBH are shown in Fig. 9a for
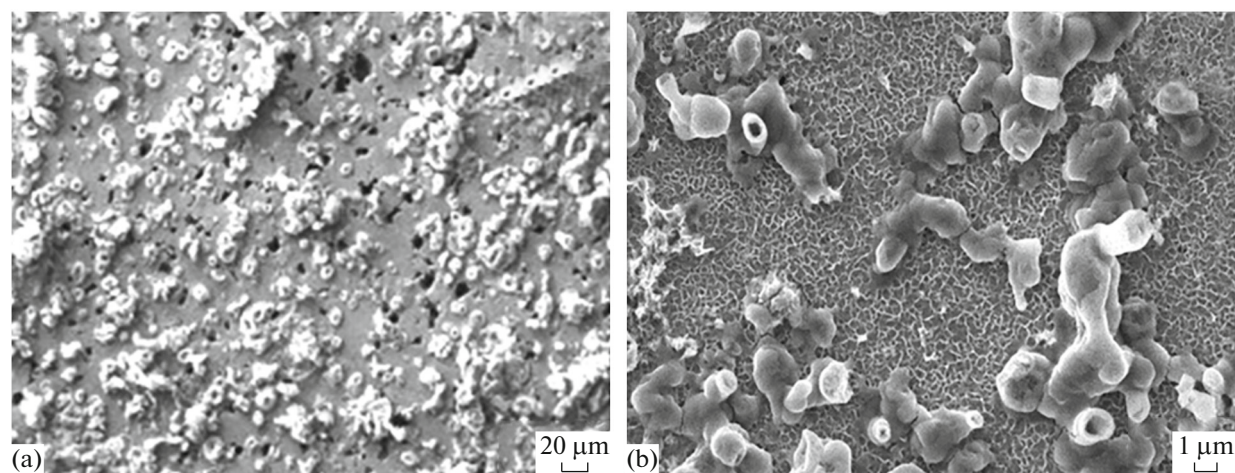
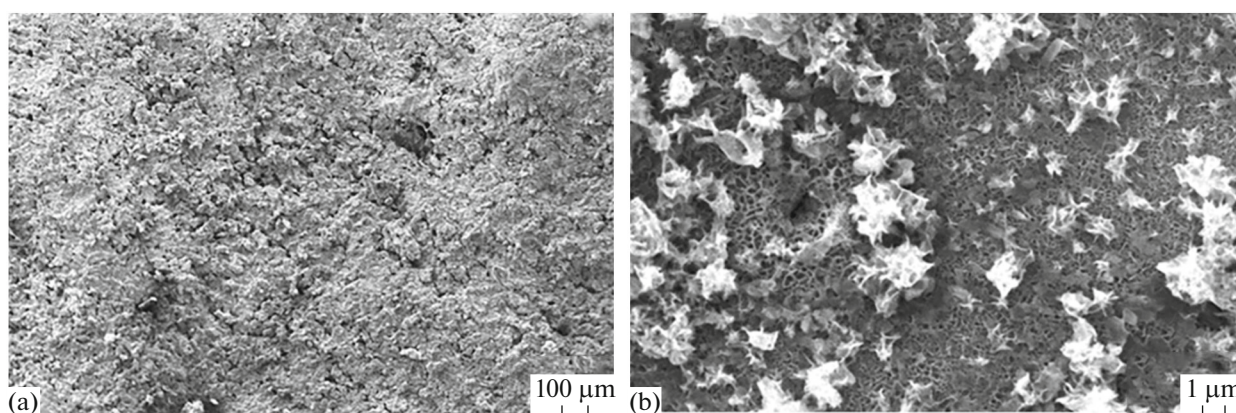**Fig. 9.** SEM images of MS specimens in: (a) 0.5 M HCl, and (b) 0.5 M HCl with 2.5×10^{-4} M of HNBH.

Fig. 10. SEM images of MS specimens in: (a) 0.5 M H_2SO_4, and (b) 0.5 M H_2SO_4 with 2.5×10^{-4} M HNBH.

HCl and Fig. 10a for H_2SO_4. After adding HNBH, the MS surface has become smoother and this shows a surface film of HNBH is formed.

CONCLUSIONS

(1) HNBH has the ability to inhibit both the anodic and cathodic reactions to some extent, thereby mainly acting as mixed type of inhibitor.

(2) The inhibition efficiency of HNBH increases with an increase in the concentration of the inhibitor and reduces with an increase in temperatures in both 0.5 M HCl and H_2SO_4.

(3) Good inhibition efficiency (around 80%) was obtained at the HNBH concentration of 2.5×10^{-4} M in both 0.5 M HCl and H_2SO_4 at all studied temperatures.

(4) The adsorption of HNBH on the MS surface follows Langmuir's adsorption isotherm.

(5) Activation and thermodynamic parameters showed that the adsorption of HNBH is mainly through physisorption in 0.5 M HCl and strong adsorption in 0.5 M H_2SO_4.

(6) There is a good correlation between EIS and Tafel polarization results.

ABBREVIATIONS

MS, mild steel; HNBH, 4-hydroxy *n*-[2-methoxy naphthalene methylidene] benzohydrazide; SEM, scanning electron microscope; EIS, electrochemical impedance spectroscopy; HCl, hydrochloric acid; H_2SO_4, sulphuric acid; PDP, potentiodynamic polarization; OCP, open-circuit potential; E_{corr}, corrosion potential; i_{corr}, corrosion current density; CR, corrosion rate; %IE, percentage inhibition efficiency; θ, surface coverage; CPE, constant phase element.

would also like to thank Dr. Padmalatha Rao for the fruitful discussion and support given during the preparation of the manuscript.

CONFLICT OF INTEREST

REFERENCES

1. Prabhu, R.A., Venkatesha, T.V., Shanbhag, A.V., Praveen, B.M., et al., Quinol-2-thione compounds as corrosion inhibitors for mild steel in acid solution, *Mater. Chem. Phys.,* 2008, vol. 108, p. 283.

2. El-Etre, A.Y., Inhibition of C-steel corrosion in acidic solution using the aqueous extract of zallouh root, *Mater. Chem. Phys.,* 2008, vol. 108, p. 278.

3. Pierre, R.R., *Corrosion Engineering Principles and Practice,* New York: McGraw Hill, 2008, 2nd ed.

4. Mercer, A.D., Corrosion inhibition: Principles and practice, in *Corrosion Control,* Shreir, L.L., Jarman, R.A., and Burstein, G.T., Eds., Oxford, UK: Butterworth Heinemann, 1994.

5. Revie, W., *Uhlig's Corrosion Handbook,* New York: Wiley Interscience, 2000, 2nd ed.

6. Saliyan, R. and Adhikari, V., Quinolin-5-ylmethylene-3-{[8-(trifluoromethyl)quinolin-4-yl]thio} propano-hydrazide as an effective inhibitor of mild steel corrosion in HCl solution, *Corros. Sci.,* 2008, vol. 50, p. 55.

7. Mohan, P., Arunsunai, K.K., Paruthimal, K.G., and Muralidharan, V.S., N'-(4-Methoxy benzylidene)benzo hydrazide as effective corrosion inhibitor for mild steel in 1M HCl, *Asian. J. Chem.,* 2012, vol. 24, p. 5821.

8. Fouda, A.S., Mohamed, M.T., and Soltan, M.R., Role of some benzo hydrazide derivatives as corrosion inhibitors for carbon steel in HCl solution, *J. Electrochem. Sci. Technol.,* 2013, vol. 4, p. 61.

9. Yadav, M., Sinha, R.R., Kumar, S., Bahadur, I., et al., Synthesis and application of new acetohydrazide derivatives as a corrosion inhibition of mild steel in acidic medium: Insight from electrochemical and theoretical studies, *J. Mol. Liq.,* 2015, vol. 208, p. 322.

10. Larabi, L., Harek, Y., Benali, O., and Ghalemb, S., Hydrazide derivatives as corrosion inhibitors for mild steel in 1M HCl, *Prog. Org. Coat.,* 2005, vol. 54, p. 256.

11. Khaled, K.F., Elhabib, O.A., El-Mghraby, A., Ibrahim, O.B., et al., Inhibitive effect of thiosemicarbazone derivative on corrosion of mild steel in hydrochloric acid solution, *J. Mater. Environ. Sci.,* 2010, vol. 3, p. 139.

12. El-Shafei, A.A., Moussa, M.N.H., and El-Far, A.A., The corrosion inhibition character of thiosemicarbazide and its derivatives for C-steel in hydrochloric acid solution, *Mater. Chem. Phys.,* 2001, vol. 70, p. 175.

13. Saliyan, R. and Adhikari, V., Corrosion inhibition of mild steel in acid media by quinolinylthiopropanohydrazones, *Indian J. Chem. Technol.,* 2009, vol. 16, p. 162.

14. Goulart, C.M., Souza, A.E., Huitle, C.A.M., Rodrigues, C.J.F., et al., Experimental and theoretical evaluation of semicarbazones and thiosemicarbazones as organic corrosion inhibitors, *Corros. Sci.,* 2013, vol. 67, p. 281.

15. Abd Ei-Rehim, S.S., Ibrahim, M.A.M., and Khaled, K.K., 4-Aminoantipyrine as an inhibitor of mild steel corrosion in HCl solution, *J. Appl. Electrochem.,* 1999, vol. 29, p. 593.

16. Khaled, K.F., Experimental and theoretical study for corrosion inhibition of mild steel in hydrochloric acid solution by some new hydrazine carbodithioic acid derivatives, *Appl. Surf. Sci.,* 2006, vol. 252, p. 4120.

17. De Oliveira, R.B., de Souza-Fagundes, E.M., Soares, R.P.P., Andrade, A.A., et al., Synthesis and antimalarial activity of semicarbazone and thiosemicarbazone derivatives., *Eur. J. Med. Chem.,* 2008, vol. 43, no. 9, p. 1983. https://doi.org/10.1016/j.ejmech.2007.11.012

18. Uhlig, H.H. and Revie, R.W., *Corrosion and Corrosion Control,* Hoboken, New Jersey: John Wiley, 2008, 4th ed.

19. Shetty, D., Kumari, P.P., Rao, S.A., and Shetty, P., Anticorrosion behaviour of a hydrazide derivative on 6061 Al 15%(v) SiC(P) composite in acid medium: experimental and theoretical calculations, *J. Bio- Tribo-Corros.,* 2020, vol. 6, p. 59.

20. Yudhistira, R., Kumari, P., Sunil, D., Shetty, P., et al., Attenuation of acid corrosion of mild steel using a novel organic dye: Electrochemical and surface measurements, *Surf. Eng. Appl. Electrochem.,* 2019, vol. 55, p. 443.

21. Kumari, P.P., Shetty, P., and Rao, S.A., Electrochemical measurements for the corrosion inhibition of mild steel in 1 M hydrochloric acid by using an aromatic hydrazide derivative, *Arab. J. Chem.,* 2014, vol. 9, p. 1878.

22. Kumari, P., Shetty, P., Rao, S.A., and Sunil, D., Inhibition behaviour of 2-[(2-methylquinolin-8-yl)oxy] acetohydrazide on the corrosion of mild steel in hydrochloric acid solution, *Trans. Indian. Inst. Met.,* 2017, vol. 70, p. 1139.

23. Li, W., He, Q., and Pei, C., Experimental and theoretical investigation of the adsorption behaviour of new triazole derivatives as inhibitors for mild steel corrosion in acid media, *Electrochim. Acta,* 2007, vol. 52, p. 6386.

24. Khaled, K.F. and Al-Qahtani, M.M., The inhibitive effect of some tetrazole derivatives towards Al corrosion in acid solution: Chemical, electrochemical and theoretical studies, *Mater. Chem. Phys.,* 2009, vol. 113, p. 150.

25. Mansfeld, F., Lin, S., Kim, K., and Shih, H.J., Pitting and surface modification of SIC/Al, *Corros. Sci.*, 1987, vol. 27, p. 997.

26. Li, W., He, Q., and Jhang, S., Some new triazole derivatives as inhibitors for mild steel corrosion in acidic medium, *J. Appl. Electrochem.,* 2008, vol. 38, p. 289.

27. Kumari, P., Shetty, P., and Rao, S.A., Corrosion inhibition effect of 4-hydroxy-N-[E-(1*H*-indole-2-ylmethylidene)] benzohydrazide, *Int. J. Corros.,* 2014, vol. 2014, id. 256424.

28. Kumar, P. and Shetty, A.N., Electrochemical investigation on the corrosion of 18%Ni M250 grade maraging steel under welded condition in sulfuric acid medium, *Surf. Eng. Appl. Electrochem.,* 2013, vol. 49, p. 253.

29. Anbarasi, C.M. and Auxilia, A.J., Surface modification of carbon steel by hexanesulphonic acid−Ni^{2+} system

and its corrosion study, *Int. J. Chem. Tech. Res.,* 2016, vol. 9, p. 218.

30. Raja, A.S. and Prathipa, V., Experimental study of inhibition effect, synergistic effect and antagonistic behaviour of L-phenylalanine − ZnSO4 at pH − 7.2 and isoelectric point (pH − 5.9) on carbon steel in aqueous solution, *Int. J. Chem. Tech. Res.,* 2015, vol. 8, p. 134.

31. Bentiss, F., Lebrini, M., and Lagrenee, M., Thermodynamic characterization of metal dissolution and inhibitor adsorption processes in mild steel/2,5-bis(*n*-thienyl)-1,3,4-thiadiazoles/hydrochloric acid system, *Corros. Sci.,* 2005, vol. 47, p. 2915.

32. Oguzie, E.E., Njoku, V.O., Enenebeaku, C.K., Akalezi, C.O., et al., Effect of hexamethylpararosaniline chloride (crystal violet) on mild steel corrosion in acidic media, *Corros. Sci.,* 2008, vol. 50, p. 3480.

33. Migahed, M.A., Mohammed, H.M., and Al-Sabagh, A.M., Corrosion inhibition of H-11 type carbon steel in 1M hydrochloric acid solution by N-propyl amino lauryl amide and its ethoxylated derivatives, *Mater. Chem. Phys.,* 2003, vol. 80, p. 169.

34. Hosseini, M.S., Mertens, F.L., and Arshadi, M., Synergism and antagonism in mild steel corrosion inhibition by sodium dodecylbenzenesulphonate and hexamethylenetetramine, *Corros. Sci.,* 2003, vol. 45, p. 1473.

35. Bentiss, F., Traisnel, M., and Lagrenee, M., Influence of 2,5-bis(4-dimethylaminophenyl)-1,3,4-thiadiazole on corrosion inhibition of mild steel in acidic media, *J. Appl. Electrochem.,* 2001, vol. 31, p. 41.

36. Singh, A.K. and Quraishi, M.A., Effect of cefazolin on the corrosion of mild steel in HCl solution, *Corros. Sci.,* 2010, vol. 52, p. 152.

37. Popova, A., Sokolova, E., Raicheva, S., and Christov, M., AC and DC study of the temperature effect on mild steel corrosion in acid media in the presence of benzimidazole derivatives, *Corros. Sci.*, 2003, vol. 45, p. 33.

38. Mallaiya, K., Subramaniam, R., Srikandan, S.S., Gowri, S., et al., Electrochemical characterization of the protective film formed by the unsymmetrical Schiff's base on the mild steel surface in acid media, *Electrochim. Acta,* 2011, vol. 56, p. 3857.

39. Popova, A., Christov, M., Raicheva, S., and Sokolova, E., Adsorption and inhibitive properties of benzimidazole derivatives in acid mild steel corrosion, *Corros. Sci.*, 2004, vol. 46, p. 1333.

40. de Oliveira, R.B., de Souza-Fagundes, E.M., Soares, R.P.P., Andrade, A.A., et al., Synthesis and antimalarial activity of semicarbazone and thiosemicarbazone derivatives, *Eur. J. Med. Chem.,* 2008, vol. 43, p. 1983.